Diamagnetic levitation enhances growth of liquid bacterial cultures by increasing oxygen availability

Dijkstra, C.E. , Larkin, O.J. , Anthony, P. , Davey, M.R. , Eaves, L. , Rees, C.E.D. and Hill, R.J.A.

Original citation & hyperlink:
Dijkstra, C.E. , Larkin, O.J. , Anthony, P. , Davey, M.R. , Eaves, L. , Rees, C.E.D. and Hill, R.J.A. (2011) Diamagnetic levitation enhances growth of liquid bacterial cultures by increasing oxygen availability. *Journal of the Royal Society Interface, volume 8* (56): 334-344.
http://dx.doi.org/10.1098/rsif.2010.0294

Note: Supplementary data for this article is available from http://rsif.royalsocietypublishing.org/content/8/56/334/suppl/DC1.

Diamagnetic levitation enhances growth of liquid bacterial cultures by increasing oxygen availability

Camelia E. Dijkstra[1], Oliver J. Larkin[1], Paul Anthony[1], Michael R. Davey[1], Laurence Eaves[2], Catherine E. D. Rees[1], Richard J. A. Hill[*,2]

[1] School of Biosciences, University of Nottingham, Sutton Bonington Campus, Loughborough, LE12 5RD, UK.

[2] School of Physics and Astronomy, University of Nottingham, Nottingham, NG7 2RD, UK.

* email: richard.hill@nottingham.ac.uk.

Diamagnetic levitation is a technique that uses a strong, spatially-varying magnetic field to reproduce aspects of weightlessness, on the Earth. We used a superconducting magnet to levitate growing bacterial cultures for up to 18 hours, to determine the effect of diamagnetic levitation on all phases of the bacterial growth cycle. We find that diamagnetic levitation increases the rate of population growth in a liquid culture and reduces the sedimentation rate of the cells. Further experiments and microarray gene analysis show that the increase in growth rate is due to enhanced oxygen availability. We also demonstrate that the magnetic field that levitates the cells also induces convective stirring in the liquid. We present a simple theoretical model, showing how the paramagnetic force on dissolved oxygen can cause convection during the aerobic phases of bacterial growth. We propose that this convection enhances oxygen availability by transporting oxygen around the liquid culture. Since this process results from the strong magnetic field, it is not present in other weightless environments, e.g. in Earth orbit. Hence, these results are of significance and timeliness to researchers considering the use of diamagnetic levitation to explore effects of weightlessness on living organisms and on physical phenomena.

Keywords: diamagnetic levitation, bacterial growth, convection, sedimentation, simulated microgravity, weightlessness

1. INTRODUCTION

It is important to understand how weightlessness influences bacterial behaviour, not only for the health of astronauts, but also for the long-term future of space exploration (Cogoli 2006). Earth-based techniques can simulate aspects of a microgravity environment, but are either time-limited to a few seconds or minutes (drop towers, parabolic flights and sounding rockets), or use rotation to time-average the gravity vector to zero, which can introduce artefacts due to the rotating reference frame (clinostats, random positioning machine) (van Loon 2007).

Here, we use the diamagnetic force induced by a strong, spatially-varying magnetic field to balance the force of gravity (Beaugnon & Tournier 1991, Berry & Geim 1997, Valles et al. 1997, Beaugnon et al. 2001, Simon & Geim 2000). Just as the centrifugal force balances the gravitational force on an orbiting spacecraft, the diamagnetic force opposes the force of gravity on a levitating object. The potential of diamagnetic levitation as a laboratory-based tool to investigate the effects of weightlessness on living organisms was first demonstrated by Valles et al. (1997), who studied levitating frog embryos, and by Berry and Geim (1997) who levitated a live frog. Liu et al. (2010) recently demonstrated levitation of a live mouse. In common with all ground-based techniques to simulate weightlessness, there are effects introduced by diamagnetic levitation that are not present in a weightless environment. For the first time, we critically assess the effect of diamagnetic levitation on a growing bacterial culture in liquid, over an 18 hour period. We use a superconducting magnet to levitate the culture.

Guevorkian and Valles (2006) reported that *Paramecia* change their swimming behaviour in magnetically-altered effective gravity, in response to the altered buoyancy of the cells. Coleman *et al*. (2007) investigated the effect of magnetic levitation on growth and cell cycle changes in wild type yeast cells, concluding that neither the growth nor the cell cycle was affected by the magnetic field when cells were levitated, but that growth was reduced at increased effective gravity. Some selective effects were seen on cells with specific mutation in transcription factors, known to mediate responses to environmental stresses such as gravity and shear stress, indicating that adaptive gene expression was required for the cells to be able to grow normally. Our

previous experiments on magnetically levitated *Arabidopsis thaliana* cell cultures have also shown that adaptive responses occur, again detected by changes in the expression of transcription factors. In this case, the adaptations were similar to those seen when cells experienced simulated weightlessness in a random positioning machine (Babbick et al. 2007). (Wilson et al. (2007) have also shown that space flight alters bacterial gene expression and virulence, in this case due to a decrease in the levels of the global gene regulator Hfq, again indicating the need for adaptation to the conditions experienced during growth in a weightless environment.)

Here we show that magnetic levitation of bacteria in a liquid culture increases the rate of population growth and the final cell density of the culture. We investigate the mechanism leading to this enhancement.

2. INITIAL HYPOTHESIS

For these experiments, we chose *Escherichia coli* and *Staphylococcus epidermidis* as examples of human commensal bacteria, and as representatives of the Gram-negative and Gram-positive groups, respectively. We used a specially-designed 17 Tesla superconducting solenoid with a closed-circuit cryogenic system, to levitate samples of bacterial culture in liquid nutrient broth. The magnet has a vertical bore. The temperature of the bore was kept at 37°C by forced air flow. Using a superconducting magnet to levitate biological organisms and material (Ikehata et al. 2003, Glade et al. 2006, Coleman et al. 2007, Babbick et al. 2007, Qian et al. 2009), rather than a resistive magnet is attractive because we can levitate for periods much longer than can be obtained, economically, using a resistive magnet.

2.1 Effective gravity acting on the liquid culture medium

Water, being diamagnetic, is repelled from the strong magnetic field at the centre of the solenoid. The liquid levitates where the magnetic force balances the gravitational force, approximately 75-80mm above the geometric centre of the solenoid, depending on the solenoid current (Hill & Eaves 2008, 2010). Following Valles et al. (1997), we define the effective gravity acting on the water as $\Gamma_z = \chi_w B B_z' / (\rho_w \mu_0) - g$, where B and $B_z' = \partial B / \partial z$ are the magnitude of the magnetic field and the magnetic field gradient, respectively; $\chi_w = -9 \times 10^{-6}$ (S.I. units) and $\rho_w = 1000\ \mathrm{kg\ m^{-3}}$ are the volume

magnetic susceptibility and density of water, respectively; $g = 9.8$ ms^{-2} is the gravitational acceleration at the Earth's surface and $\mu_0 = 4\pi \times 10^{-7}\mathrm{NA}^{-2}$. At the levitation point $\Gamma_z = 0$. Since the culture medium is composed mostly of water, it levitates at the same position, under the same conditions. Notice that a *positive* value of Γ_z indicates a net *upward* force, and a *negative* value of Γ_z indicates a net *downward* force. A more detailed discussion of effective gravity and the variation in Γ near the levitation point can be found in Appendix S1, in the Electronic Supplementary Material (ESM).

2.2 Effective gravity acting on the cells

Whether an individual cell floats or sinks in the liquid culture medium depends on Archimedes' principle, i.e. on the difference between the cell's weight and the weight of fluid displaced by the cell. In a weightless environment, e.g. in an orbiting spacecraft, both weights are zero, so the cells are neutrally buoyant. We express the net force acting on the cell, including buoyancy forces, as an effective gravity: $\Gamma_z^{(c)} = \Delta\chi BB_z'/(\rho_c\mu_0) - g\Delta\rho/\rho_c$, where $\Delta\chi = \chi_c - \chi_w$ and $\Delta\rho = \rho_c - \rho_w$. Here, χ_c is the spatially-averaged volume magnetic susceptibility of the cell and ρ_c is the spatially-averaged ('buoyant') density of the cell (i.e. its mass divided by its volume). See Appendix S2.1 in the ESM for the derivation and additional discussion.

For neutral buoyancy, we require the net force acting on the cell to be zero; that is, we require $\Gamma_z^{(c)} = 0$. Outside the magnet, $\Gamma_z^{(c)} \approx -0.09g$, since the buoyant density of the bacterial cells is $\rho_c \approx 1090\ \mathrm{kg\,m^{-3}}$ (Kubitschek 1986); hence we expect the cells to sediment in the culture medium, outside the magnet. We now consider whether the diamagnetic force on the cells and on the fluid can prevent the cells from sinking. We estimate $\Delta\chi = -(8 \pm 3) \times 10^{-7}$ experimentally by measuring the levitation position in the bore (Tanimoto et al. 2005); most of the experimental error in this measurement is due to uncertainty in the water content of the bacterial pellet. From this result, we estimate that $\Gamma_z^{(c)} = (-0.01 \pm 0.03)g$ at the levitation point of the culture medium. This analysis suggests that it is *possible* to achieve a pseudo-weightless condition in the magnetically levitated bacterial culture, in the sense that the fluid medium is weightless and the cells are simultaneously neutrally buoyant in the fluid ($\Gamma_z^{(c)} \approx 0g$).

2.3 Estimate of the effect of levitation on the sedimentation rate of the cells

Based on our experimental measure of $\Delta\chi$, we estimate that the sedimentation rate should be reduced to (10±30)% of the rate exhibited outside the magnet. The negative percentage encompassed by the uncertainty in this value indicates that our estimate includes the possibility that the cells will float to the surface, rather than sink. We have expressed the sedimentation rate as a percentage of the 1 g control rate, rather than an absolute value, since the rate is dependent on the cell size. The calculation is outlined in Appendix S2.2 (ESM).

3. CONTROLS

We use culture volumes > 1 ml to allow for sampling during the experiment and to ensure that the culture volume is not significantly affected by evaporation. Strong magnetic fields of order 10 T are required to magnetically levitate culture volumes of this size; in our experiments, $B = 12.3$ T at the levitation point. There is evidence that B fields of this strength affect biological organisms at the cellular level. For example, striking changes were observed in the orientation of cell-division cleavage planes in developing frog embryos in a static field $B \sim 1$ T (Denegre et al. 1998, Valles 2002). Stresses can arise from a magnetic torque resulting from anisotropy in the magnetic susceptibility of structures (Valles 2002, Hill et al. 2007). The significance of these forces depends on whether the energy associated with such forces is larger than the thermal energy scale. Another possibility is that the magnetic field can affect biochemical kinetics (Steiner & Ulrich 1989). Internal stresses in a biological cell can also be altered in a *gradient* magnetic field, due to variations in the magnetic susceptibility of the cell's constituents. Valles et al. (1997) performed experiments on magnetically levitated frog embryos, concluding that levitation *reduced* the gravity-induced internal stresses within the cell.

We shall not analyse these possibilities in further detail here. However, by using a control sample placed at the centre of the solenoid coil, enclosing the $\Gamma = 1g$ point, we can distinguish experimentally between the effects of magnetic forces that are proportional to the field-field gradient product BB_z', and magnetic effects that depend only on B (Valles et al. 1997, 2005). As an additional control, a sample container was also placed below the centre of the solenoid, enclosing the $\Gamma = 2g$ point, where gravity

and the magnetic force are additive, and $B = 12.3$ T. For convenience, we label the sample containers "0g*", "1g*" and "2g*" corresponding to the effective gravity enclosed by each container; the asterisk on the label indicates the sample is in a strong magnetic field, either 16.3 T at 1g* or 12.3T at 0g* and 2g*. The variation of Γ in the 0g* container is discussed in Appendix S1 and shown in Fig. S1 (ESM). We use the label "1g" to indicate the control sample, grown outside the magnet.

4. REDUCED SEDIMENTATION RATE

To test our hypothesis that levitation inhibits sedimentation of the bacteria in the liquid culture, we used *E. coli* transformed to a green fluorescence phenotype (GFP) to visualize the distribution of cells within the culture vessel. Cultures were exposed to the magnetic field, one at each of the positions 0g*, 1g* and 2g*, simultaneously at a temperature of 37 °C for 18 h. Figure 1 shows that the sedimentation rate of cells was reduced in the 0g* position, compared to the 1g* sample, indicated by the higher optical density of the 0g* culture throughout the tube. Sedimentation at the 2 g* position was enhanced compared to the 1g* sample: the supernatant was almost clear, with the cells forming a layer on the bottom of the vessel. In separate experiments, the optical density (OD_{600nm}) OD_1 of the supernatant was measured to determine the cell density remaining in suspension. A second optical density measurement OD_2 was taken immediately after vortexing each sample to determine the OD value of an evenly suspended culture. The fraction of sedimented cells after the 18 h period is $S = 1 - OD_1/OD_2$, which is proportional to the sedimentation speed and the time of incubation. The OD_1 of the 0g* culture was higher than that of the 1g* sample in the magnet, and the 1g control outside the magnet. The fraction of sedimented cells at the 0g* position was $S(0g^*) = 0.38 \pm 0.06$, whereas in the 1g* control, $S(1g^*) = 0.54 \pm 0.01$. In the 1 g control outside the magnet, $S(1g) = 0.50 \pm 0.01$. The uncertainties are one standard deviation. These results indicate that significantly more bacteria remain in suspension in 0g* than in the 1g and 1g* samples. There is a small difference between $S(1g)$ and $S(1g^*)$ which may be due to some mixing as the 1g* sample is withdrawn from the magnetic field. The ratios $S(0g^*)/S(1g)$ and $S(0g^*)/S(1g^*)$ lie just outside the range we estimate from the Stokes drag analysis. This suggests that another mechanism may be influencing the apparent sedimentation rate. In section 7, we discuss experiments in which we image the

samples *in-situ*. These experiments show that the gradient magnetic field can cause convective stirring where there is a gradient in the dissolved oxygen concentration.

5. EFFECT ON GROWTH PHASES

To investigate the effect of levitation on the growth of these cultures, cell density was measured as a function of time by taking optical density (OD_{600nm}) measurements at approximately 1 h intervals to determine growth rate and lag time. Cultures of untransformed *E. coli* and *S. epidermidis* were grown within the magnet at the three different positions (0*g**, 1*g** and 2*g**). In addition, control samples were incubated outside the magnet (1*g*). Cultures within the magnet bore and the 1*g* control sample were incubated statically at 37 °C. Each sample was mixed prior to measurement. Figure 2 shows that for both *E. coli* and *S. epidermidis* cultures grown at 0*g**, an overall enhancement of growth was apparent compared to the static (1*g*) control cultures. No difference in the lag phase or initial growth rate was observed when cultures had low cell density. However, the cultures at 1*g** and 2*g** and the 1*g* control all showed a lower initial growth rate than the 0*g** cultures (Fig. 2). The final cell density in the 0g* samples was approximately 1.5 times that of the other cultures. These results are reproducible and statistically significant. The growth in the 1g control is comparable to that in the 1g* sample, demonstrating that, in the absence of a magnetic field gradient, the magnetic field has no observable effect on the growth. For comparison, we performed an experiment on a *shaken* culture outside the magnet, in which we expect the liquid to be fully aerated. We found that, although growth was enhanced at 0*g** compared to all the *static* cultures, it was not as high as that achieved by the aerated culture outside the magnet (Tables 1a and b). Liquid loss via evaporation was insignificant because the cultures vessels were air tight.

6. OXYGEN AVAILABILITY LIMITING GROWTH

6.1 Experiments with perfluorodecalin

The lower growth rate in the static cultures, compared to the shaken cultures, suggests that availability of O_2 is limiting growth in the static cultures. To test this experimentally, we performed experiments in tubes containing different volumes of liquid medium *V*. We also performed experiments in tubes of different diameter, to see the effect of varying the area of the air-liquid interface *A*. We found a clear positive

relationship between final cell number density and A/V (Fig. 3). This result lends weight to the hypothesis that the availability of O_2 is limiting growth in these experiments, since the O_2 flux across the air/water interface is proportional to A and the O_2 concentration of the liquid resulting from this flux is inversely proportional to V. To confirm that availability of O_2 is limiting growth, cultures were oxygenated from the bottom of the vessel by using the artificial gas carrier perfluorodecalin (PFC). PFC has a high saturation capacity for O_2, and is both more dense than, and immiscible with, water; it forms a discrete layer at the bottom of the culture and has been shown previously to enhance growth of bacterial cultures (Atlung et al. 1997). All the samples with PFC showed enhanced growth compared to samples without PFC. Under these conditions, the final cell number density of the $0g^*$ sample was as high as in the aerated cultures and the $1g^*$, $2g^*$ and $1g$ cultures all grew as well as the $0g^*$ sample without PFC (Tables 1a and b). This confirms that lack of O_2 is limiting growth in the lower region of the static cultures. Further, these results suggest a reason for the $0g^*$ growth enhancement: magnetic levitation increases the availability of O_2. We test this hypothesis by a gene expression study in the following section. The fact that the growth rate of the $1g^*$ culture is increased by inclusion of the PFC layer, indicates that the magnetic field does not limit growth in these experiments.

6.2 Changes in gene expression

In adapting to different growth conditions, *E. coli* alters the composition of its respiratory pathways, changing the amount of different terminal oxidases to optimize its respiratory chain according to the substrates present and the physiological needs of the cell. Cytochrome b_o, encoded by the *cyoABCDE* operon, operates at high oxygen concentration and has low affinity for oxygen. Expression of the *cyo* operon is decreased under anaerobic conditions by the global anaerobic regulators ArcA and Fnr (Cotter & Gunsalus 1992). The AppB cytochrome bd-type oxidase has a high oxygen affinity and is encoded in an operon with AppA (pH 2.5 acid phosphatase). Their expression is regulated by AppY and stress-response sigma factor RpoS under microaerobic conditions, when AppB may be required for efficient electron transport (Atlung et al. 1997). We used microarray-based gene expression profiling to investigate the response to O_2 depletion. RNA was extracted from each of the *E. coli* cultures grown under the different test conditions when the cells reached mid-

exponential growth phase (OD_{600nm}= 0.5) and samples analyzed on an *E. coli* oligonucleotide array (Table 2). Expression of genes in the *cyo* operon were consistently ~2-fold up-regulated in the 0*g** samples compared to all other static samples. No significant difference in expression of these genes was detected between the 0*g** static culture and the 1g aerated culture. The opposite pattern was seen for genes in the *app* operon; the expression of these genes was enhanced at 2*g**. Additionally, the anaerobic growth regulator *fnr* was down-regulated in the 0*g** compared to 2*g** sample. In general, genes known to be associated with anaerobic adaptation were more highly expressed in samples with the lowest growth. Changes in expression of *cyoA* and *appB* were also confirmed by qRT-PCR analysis and showed that the expression of the *cyoA* gene was enhanced at 0*g** compared with the control (Table 3), with the 1.5-fold change observed being similar to results obtained from the microarray analysis. The expression of the *appB* gene was down-regulated at 0*g** but was enhanced at the 2*g** position compared with the control by approximately 2-fold. Importantly, no differences in level of expression of these cytochromes were found between the 1*g** and 1*g* static samples, indicating that their expression was not influenced by the magnetic field or by differences in distribution of other nutrients influenced by the magnetic field, but rather by differences in oxygen availability under the different test conditions.

7. MAGNETICALLY-INDUCED CONVECTION

One might speculate that the increase in oxygen availability in the levitated (0*g**) sample may be due to the observed reduction in the rate of sedimentation. This allows bacteria to remain closer to the surface where the liquid is enriched by oxygen diffusing across the air-liquid interface. Whilst this is a plausible hypothesis, we also investigated whether previous studies of magnetically-induced convection in water could be relevant (Ueno & Iwasaka 1994, Hirota et al. 2000, Kishioka et al. 2000, Kitazawa et al. 2002, Iwasaka et al. 2003, Ikehata et al. 2003, Peng et al. 2004). Molecular oxygen is paramagnetic and is attracted to a magnetic field: molecular oxygen above the solenoid is pulled towards the centre of the solenoid, where the field is largest. This force enhances the buoyancy of objects immersed in a paramagnetic fluid (Ikezoe et al. 1998, Catherall et al. 2003, 2005; Lopez-Alcaraz et al. 2007). Although the paramagnetism of O_2 at room temperature is weaker than that of liquid

oxygen, the paramagnetic force on the O_2 molecules in air in the bore of our superconducting magnet is nevertheless significant due to the large gradient magnetic field. This is easily demonstrated by levitating a droplet of water in the magnet: in air, the droplet levitates 6 mm higher than its position in nitrogen gas (at the same temperature and pressure) due to the additional buoyancy force provided by the paramagnetic force on the O_2 molecules in the air (Hill & Eaves 2010). Ueno (1989) showed that the paramagnetic force on O_2 in the air is strong enough to extinguish a burning candle with a 1.5 T electromagnet. O_2 dissolved in the liquid culture medium, is similarly attracted by the magnetic field (Aoyagi et al. 2006). Since O_2 in the liquid is consumed by the bacteria and replaced at the liquid-air interface (from the O_2 in the air above the liquid), an O_2 concentration gradient results, producing a corresponding gradient in the magnetic force density. Analogous magnetic effects on convection have been observed in crystal growth experiments in high gradient magnetic fields, resulting from a concentration gradient of solute (Poodt et al. 2005, Heijna 2007).

7.1 Theory

We now consider whether this force gradient can cause convection of the liquid medium by comparison with convection driven by a temperature-dependent density gradient, which is well understood. We define an *effective liquid density* P such that the net vertical force on a volume V of liquid in the magnetic field $F_z = \chi V B B_z'/\mu_0 - \rho_w V g$ can be written $F_z = PV\Gamma$, where $P = \rho_w + (\chi - \chi_w)BB_z'/(\Gamma\mu_0)$; ρ_w and χ are the liquid density (approximately the same as water) and the volume magnetic susceptibility, respectively. For simplicity, we consider the forces on-axis only, where $\Gamma = \Gamma_z$. Importantly, note that χ depends on the concentration C (here, measured in molecules per m^3) of dissolved oxygen in the liquid: $\chi(C) = \chi_w + \gamma C$, where $\gamma = 43 \times 10^{-9} m^3 mol^{-1}/N_A$ is the molecular magnetic susceptibility of O_2 at room temperature (Weast, ed., 1972); N_A is Avagadro's number. Therefore, the effective density of the liquid P depends on the concentration of dissolved oxygen C. A gradient in the oxygen-dependent effective density can give rise to convection in an entirely analogous way to a temperature-dependent density gradient. In the text-book problem of Rayleigh-Bénard (RB) convection (e.g. Faber 1995), a temperature gradient is established between a hot plate at the base of the liquid and a cold plate at the top. The difference in density between the warm liquid near the base and the cooler liquid at the top

causes the system to become unstable to convection when the temperature gradient exceeds a critical value, determined by the Rayleigh number. For example, for 20°C water between plates separated by 1 cm, we expect to observe convection when the temperature gradient exceeds approximately 0.15 K cm^{-1}. We now consider an analogous configuration, which will allow us to use the existing theory on RB convection to provide an insight into the present problem: we assume for the moment that the bacteria lie in a layer at the bottom of the vessel, consuming O_2, so that, in equilibrium, C decreases linearly from C_i at the liquid-air interface to C_b at the container bottom. We can define a Rayleigh number for this configuration, in an exact analogy with the thermal convection problem,

$$\mathrm{Ra}^* = \frac{\alpha \Gamma h^3 \Delta C}{D\nu}$$

Here, $\Delta C = C_b - C_i$, $h \sim 1$ cm is the depth of the liquid, $D \sim 3 \times 10^{-9}$ m^{2}s^{-1} is the diffusivity of O_2 molecules in the medium at 37°C [approximately the same as that in water (Wilke & Chang 1955)], $\nu \sim 1 \times 10^{-6}$ m^{2}s^{-1} is the kinematic viscosity of the medium, and α is the fractional change of P with C,

$$\alpha = -\frac{1}{P}\left(\frac{\partial P}{\partial C}\right).$$

Notice that the molecular diffusivity D and the concentration difference ΔC are the analogues of the thermal diffusivity and temperature difference, respectively, in the thermal convection problem. Poodt et al. (2006) used a Ra number for analyzing the results of the similar problem of mass-transport in magnetically-levitated crystal growth, although they do not introduce the concept of effective density explicitly. We emphasize that Ra^* is not the same as the "magnetic Rayleigh number" that characterizes convection driven by temperature-induced changes in fluid magnetization (e.g. Nakamura et al. 2005). In the present problem, the O_2 concentration gradient is responsible for convection, not the temperature, which is *uniform* throughout the liquid. Since the diffusivity of O_2 in air is $\sim 1 \times 10^4$ times larger than in water (Marrero & Mason 1972), we can assume that there is a negligible O_2 concentration gradient in the air above the liquid. Hence, we assume that the

concentration of O_2 in the surface liquid is approximately the same as that in water in equilibrium with the air, which is $C_0 \sim 1 \times 10^{23}$ molecules per m^3 at 37°C (Benson & Krause 1980). At the container bottom, the bacteria consume O_2 until its concentration reaches $C_b \approx 0.01 C_0$, at which point the low O_2 concentration limits the activity of the bacteria (Chen et al. 1985) (at these cell densities, $5 \times 10^7 - 5 \times 10^9$ m^{-3}, the rate of O_2 diffusion through the liquid limits the bacterial O_2 consumption). For simplicity, we use the approximation $C_b = 0$. In the $0g^*$ position, the effective density P of the O_2-rich liquid at the surface is greater than that of the O_2-poor region below. From existing theory on RB convection, we know that this configuration is unstable above $Ra^* \sim 2000$. (Note that the culture at $2g^*$ is stable against this type of convection since the paramagnetic force on the O_2 pulls *upward* in this location.) Calculating the Ra^* number for the model system, we find that, within the $0g^*$ sample, $Ra^* > 1 \times 10^6$ on-axis. Hence, we expect our model $0g^*$ system to be unstable to convection. Although, in the experiments, a fraction of the bacteria are suspended in the liquid, as we demonstrated in section 4, and the *E. coli* are also motile, the large Ra^* number for the model $0g^*$ system suggests that convection driven by an O_2 concentration gradient could be possible under experimental conditions, too.

7.2 Experiment to test for magnetically-induced convection

We tested this hypothesis experimentally by performing growth experiments on *E. coli* including the redox dye resazurin. This blue, water-soluble, dye is reduced, irreversibly, to the pink dye resorufin by reactions associated with bacterial respiration (Guerin et al. 2001). Resorufin can itself be further reduced to the colourless hydroresorufin by the same processes. However, the second reaction is reversible by O_2 (Guerin et al. 2001). Since the dye molecules are diamagnetic, the magnetic force on each is small compared to the force on an O_2 molecule; we measured the susceptibility of the powdered dyes using the Gouy method. Therefore, we do not expect the introduction of the dye to have any effect on the convection. Figure 4 shows cultures containing the dye in the $0g^*$ and $2g^*$ positions, and in a control sample ($1g$) outside the magnet. The photographs were obtained *in situ*, 6 h after introduction of the dye. Unlike the experiment performed to measure growth, where samples were mixed prior to sampling, these static cultures were left undisturbed. Just after the dye was introduced, all samples had a uniform blue colour, but turned pink after approximately 2 h due to

bacterial aerobic respiration. The pink colour of the 1*g* control sample faded to colourless after a further 1-2 h, as the dissolved O_2 was depleted and the resorufin was further reduced. However, close to the air-liquid interface, the liquid remained pink due to O_2 diffusion across the interface, which prevented the reduction of resorufin to hydroresorufin. In contrast, the colour of the sample in the 0*g** position did not fade to colourless, remaining bright pink (including in the region at the bottom of the container), except for the appearance of two paler oval-shaped areas. Comparison with the control sample suggests that within these pale ovals, the O_2 concentration must be lower than in the rest of the fluid. We also note that the oval shapes of these regions are reminiscent of the shape of stagnant regions in thermal convection cells (Faber 1995). These two observations suggest that the concentration of dissolved O_2 *outside* the oval regions is increased by convective transport of O_2 from the relatively O_2-rich surface-liquid to the rest of the sample. The fluid within the ovals stagnates, as is typical in a convection cell, and therefore O_2 levels in these regions are depleted by bacterial respiration, allowing resorufin to be reduced to its colourless form. Since the paramagnetic force on the O_2 in the 2g* sample acts upward, we expect these samples to be stable against paramagnetic O_2 convection. This is evident from the well-defined pink layer at the top of this container.

Since the nutrient broth contains paramagnetic metal ions, Fe^{2+}, Cu^{2+} and Mn^{2+} , in concentrations comparable to C_0, one might ask whether these ions could also give rise to convection, since the bacteria require these ions for their metabolic processes. However, Bovallius and Zacharias (1971) showed that, in nutrient broth, these ions are present at sufficient concentration to avoid rate-limiting the bacterial growth. Hence, we do not expect a significant concentration gradient of these ions to arise; we emphasise that a concentration *gradient* is required to generate convection by this mechanism. Conversely, since we have shown that O_2 depletion limits growth in our experiments, we expect a significant O_2 concentration gradient. We have shown, theoretically and experimentally, how such an O_2 concentration gradient in the magnetic field can generate convection.

A natural question to ask at this point is whether the sedimentation itself is inhibited by the paramagnetic convective stirring, rather than by diamagnetic levitation. Since we

observe an *increase* in the rate of sedimentation in the 2*g** position, this demonstrates that the diamagnetic force on the liquid and the cells does indeed have a direct effect on sedimentation (increasing the sedimentation rate in the 2*g** sample), since the liquid in this position is stable against the paramagnetically-induced convection discussed above. However, we must conclude that the convective-stirring has a significant effect on the availability of O_2 to the bacteria in the 0*g** sample, since the convective flow transports O_2 from the O_2 rich surface through the bulk of the liquid.

8. CONCLUSION

From our experimental data, we attribute the increase in bacterial growth rate and higher final cell density in the 0*g** samples to greater oxygen availability. The effect becomes enhanced at high cell density when the respiration of the bacteria rapidly depletes oxygen levels. This explanation is supported by the observations that (i) the 0*g** sample supplemented with PFC behaves as a uniformly aerated culture and (ii) the anaerobic adaptation genes were more strongly induced in the 1*g** and 2*g** cultures, confirming that they were experiencing oxygen depletion. We have shown that the diamagnetic force can directly affect the sedimentation rate of a bacterial culture. We have also demonstrated that the gradient magnetic field in the 0*g** position has a significant effect on the transport of O_2 in the liquid culture: the consumption of O_2 by the living cells and its replenishment by O_2 diffusing across the liquid-air interface can generate convection in the magnetic field, analogous to the thermal, Rayleigh-Bénard convection process. It is likely that the enhanced availability of O_2 in 0*g** is due to this latter effect. Diamagnetic levitation has the potential to be a powerful technique to study the effects of weightlessness on biological cells, to complement existing Earth-based techniques such as clinorotation and random positioning. However, for diamagnetic levitation to be a useful model of the weightless space environment, where density-driven convective transport is absent, paramagnetically-driven convection of O_2 should be prevented. One possibility is to perform experiments on anerobically metabolising organisms, or in non-liquid cultures (Beuls et al, 2009).

MATERIALS AND METHODS

Bacterial cultures

Escherichia coli K12 MG1655 and *Staphylococcus epidermidis* NCTC11047 were grown in Nutrient Broth (NB; Oxoid, UK). Gfp^+ bacteria were *E. coli* TOPO(pSB2999) [$P_{rpsJB.subitilis}$::*gfp* in pDEST R4-R3; P.J. Hill, University of Nottingham] which were grown in NB supplemented with Ampicillin (50 $\mu g ml^{-1}$). All cultures were grown at 37 °C. Aerated cultures were shaken at 150 rpm.

Experimental levitation magnet system

The superconducting solenoid has a 50 mm-diameter vertical bore, open to the laboratory at both ends (Fig. S2). A closed-cycle coolant system allows the magnet to run at high magnetic field on time scales of the order of several months. A constant mean temperature of 37°C in the bore was maintained, with variation over time <0.2°C, by temperature-regulated forced air flow with feedback control. The temperature-controlled chamber consists of an acrylic tube (length 60 cm, internal diameter 44 mm), inserted into the magnet bore, containing three specimen tubes (25mm internal diameter, 25ml capacity), one at each of the 0*g**, 1*g** and 2*g** positions (Fig. S3). The 1*g** sample is located at the centre of the coil; the 0*g** and 2*g** samples are located 75mm above and below the 1*g** position, respectively. The temperature of each sample was monitored by a thermocouple in contact with each specimen tube. The effect of magnetic field up to 17 T on the thermocouples was negligible.

Growth Experiments

Cultures were inoculated into fresh NB at an OD_{600nm} = 0.05. The growth experiments and sedimentation experiments presented in Sections 4 and 5 were performed in 25ml containers (25mm internal diameter, 50mm tall). The containers were filled with the liquid culture to a depth of 15mm. The experiments to determine the effect of the liquid surface area to volume ratio (Section 6) were performed in containers of varying sizes and culture volumes; their dimensions are summarized in Table S1. Samples were exposed to 0*g*,* 1*g** or 2*g** for varying periods of time, in the dark at 37 ± 0.1ºC. Each sample was removed from the magnet, mixed, and its cell numbers determined at approximately 1 h intervals to determine growth rate and lag time. Cell number was

determined by viable count or by optical density (OD_{600nm}). In the experiments to visualise convection (Section 7), spectrophotometer cuvettes (10mm x 10mm x 45mm) were filled with the liquid culture to a depth of 12mm and incubated at 0g*, 1g*, 2g* and 1g at 24°C; the lower temperature slowed bacterial growth to allow changes within the fluid to be visualized more easily. Resazurin was used at a final concentration of 67 mg ml^{-1} .

Perfluorocarbon (PFC)

Perfluorodecalin (Flutec® PP6) liquid was oxygenated for 20 min with 100% oxygen gas and dispensed as 4 ml aliquots in sample tubes. For growth experiments, 4 ml of bacterial suspension was overlaid on the PFC and samples exposed to altered gravity in the magnet for 16 h. The position of the sample in the magnet bore was altered to compensate for the raised height of the growth medium due to the presence of the PFC layer in the bottom of the tube. Data were analyzed using the One-way ANOVA and Tukey's pair-wise comparisons post hoc analysis with a 95% confidence interval, using SPSS software.

Microarray analysis

Samples were exposed to each test condition and cells harvested in the mid-exponential phase of growth and 4 independent replicates of each experiment were performed. Total RNA were extracted and labelled using the protocol outlined in MessageAmp™ II-Bacteria. RNA (700 ng) was labelled with 5-(3-aminoallyl)-UTP. Samples (5µg) of RNA were labelled with Cy5 using NHS-ester reactive dye packs and purified using RNeasy MinElute columns. The DNA reference samples (1µg) were labelled using the Invitrogen 'BioPrime DNA labeling System', with Cy3-dCTP. Agilent MG1655 microarray slides were hybridized at 65°C for 17 h and scanned at 5 µm resolution using the extended dynamic range (Hi 100%, Low 10%). Data were analyzed using Agilent Feature Extraction software and imported into the GeneSpring GX package, normalized per chip to 50% of signal and genes whose normalized expression levels changed 2-fold or more were identified by applying a t-test ($p = 0.05$). Differentially transcribed genes were divided into functional groups using COG and KEGG. A complete analysis of genes involved in oxidative phosporylation pathway with a significantly different level of expression is presented in Table S2.

Quantitative Real-Time RT-PCR

All qRT-PCR experiments were performed in triplicate on RNA used for microarray analysis and cDNA was synthesized from 2 µg RNA. Custom TaqMan assays for *cyoA, appB* and *envZ* genes were used (Table S3). The thermal profile employed was 50 °C for 2 min, 95 °C for 10 min, and 40 cycles of 95°C for 15 s, 60°C for 1 min. Average C_T values and standard deviation were calculated for the 3 replicates. $\Delta\Delta C_T$ was calculated by the difference between ΔC_T of test samples (0*g*,* 1*g*,* 2*g** and 1*g* aerated) and control sample (1*g* static).

Author contributions

C.E.D., O.L., R.J.A.H. and P.A. performed experiments; C.E.D., O.L., R.J.A.H., P.A., M.R.D., L.E. and C.E.D.R. designed experiments; C.E.D., O.L., C.E.D.R. and R.J.A.H. analyzed data; and C.E.D., O.L., R.J.A.H., L.E. and C.E.D.R. wrote the paper.

Acknowledgements

We thank the technical staff in the School of Physics, especially D. A. Holt, P. Smith, S. R. Booth, S. Nankervis and I. Taylor, for assistance in constructing the temperature-controlled chamber and *in situ* imaging hardware, and P. J. Hill for supplying the GFP bacteria. This work was supported by a Basic Technology Grant from EPSRC, UK; Grant Nos. GR/S83005/01 and EP/G037647/1.

References

Aoyagi S, Yano A, Yanagida Y, Tanihira E, Tagawa A, Iimoto M (2006) Control of chemical reaction involving dissolved oxygen using magnetic field gradient. *Chem Phys* 331:137–141.

Atlung T, Knudsen K, Heerfordt L, Brøndsted L (1997) Effects of sigma(S) and the transcriptional activator AppY on induction of the *Escherichia coli hya* and *cbdAB-appA* operons in response to carbon and phosphate starvation. *J Bacteriol* 179:2141–2146.

Babbick M, Dijkstra C, Larkin OJ, Anthony P, Davey MR, Power JB, Lowe KC, Cogoli-Greuter M, Hampp R (2007) Expression of transcription factors after short term exposure of *Arabidopsis thaliana* cell cultures to hypergravity and simulated microgravity (2-D/3-D clinorotation, magnetic levitation). *Adv Space Res* 39:1182-1189.

Beaugnon E, Fabregue D, Billy D, Nappa J, Tournier R (2001) Dynamics of magnetically levitated droplets. *Physica B* 294:715-720.

Beaugnon E, Tournier R (1991) Levitation of Water and Organic-Substances in High Static Magnetic-Fields. *J Phys III* 1:1423-1428.

Benson BB, Krause, Jr. D (1980) The concentration and isotopic fractionation of gases dissolved in freshwater in equilibrium with the atmosphere. 1. Oxygen. *Limnol Oceanogr* 25:662-671.

Berry MV, Geim AK (1997) Of flying frogs and levitrons. *Eur J Phys* 18:307-313.

Beuls E, Van Houdt R, Leys N, Dijkstra CE, Larkin OJ, Mahillon J (2009) Bacillus thuringiensis Conjugation in Simulated Microgravity. *Astrobiology* 9:797

Bovallius Å, Zacharias B (1971) Variations in the metal content of some commercial media and their effect on microbial growth. *Appl Microbiol* 22:260-262.

Catherall AT, Eaves L, King PJ, Booth SR (2003) Magnetic levitation: Floating gold in cryogenic oxygen. *Nature* 422:579.

Catherall AT, Lopez-Alcaraz P, Benedict KA, King PJ, Eaves L (2005) Cryogenically enhanced magneto-Archimedes levitation. *New J Phys* 7:118-128.

Chen J, Tannahill AL, Shuler ML (1985) Design of a system for the control of low dissolved oxygen concentrations: critical oxygen concentrations for Azobacter vinelandii and Escherichia coli. *Biotech and Bioeng* 27:151-155.

Cogoli A (2006) in *Fundamentals of Space Biology: Research on Cells, Animals, and Plants in Space, Space Technology Library, Vol. 18*, eds Clément G, Slenzka K (Microcosm Press, El Segundo, CA & Springer NY), pp 121-170.

Coleman CB, Gonzalez-Villalobos RA, Allen PL, Johanson K, Guevorkian K, Valles JM, Hammond TG (2007) Diamagnetic levitation changes growth, cell cycle, and gene expression of *Saccharomyces cerevisiae*. *Biotechnol Bioeng* 98:854-863.

Cotter PA, Gunsalus RP (1992) Contribution of the *fnr* and *arcA* gene-products in coordinate regulation of cytochrome-o and cytochrome-d oxidase (*cyoABCDE* and *cydAB*) genes in *Escherichia coli*. *FEMS Microbiol Lett* 91:31–36.

Denegre JM, Valles JM, Jr., Lin K, Jordan WB, Mowry KL (1998) Cleavage planes in frog eggs are altered by strong magnetic fields. *Proc Natl Acad Sci USA* 95:14729-14732.

Faber TE (1995) Fluid Dynamics for Physicists, Cambridge University Press.

Glade N, Beaugnon E, Tabony J (2006) Ground-based methods reproduce space-flight experiments and show that weak vibrations trigger microtubule self-organisation. *Biophys Chem* 121:1-6.

Guerin TF, Mondido M, McClenn B, Peasley B (2001) Application of resazurin for estimating abundance of contaminant-degrading organisms. *Lett Appl Microbiol* 32:340.

Guevorkian K, Valles JM (2006) Swimming *Paramecium* in magnetically simulated enhanced, reduced, and inverted gravity environments. *Proc Nat Acad Sci USA* 103:13051-13056.

Heijna MCR, Poodt PWG, Tsukamoto K, de Grip WJ, Christianen PCM, Maan JC, Hendrix JLA, van Enckevort WJP, Vlieg E (2007). Magnetically controlled gravity for protein crystal growth. *Appl Phys Lett* 90:264105.

Hill RJA, Sedman VL, Allen S, Williams P, Paoli M, Adler-Abramovich L, Gazit E, Eaves L, Tendler SJB (2007) Alignment of Aromatic Peptide Tubes in Strong Magnetic Fields. *Adv Mat* 19:4474-4479.

Hill RJA, Eaves L (2008) Nonaxisymmetric Shapes of a Magnetically Levitated and Spinning Water Droplet. *Phys Rev Lett* 101:234501-234504.

Hill RJA, Eaves L (2010) Vibrations of a diamagnetically levitated water droplet. *Phys Rev E* 81:056312.

Hirota N, Ikezoe Y, Uetake H, Nakagawa J, Kitazawa K (2000) Magnetic Field Effect on the Kinetics of Oxygen Dissolution into Water. *Materials Transactions, JIM* 41:976-80.

Ikehata M, Iwasaka M, Miyakoshi J, Ueno S, Koana T (2003) Effects of intense magnetic fields on sedimentation pattern and gene expression profile in budding yeast. *J Appl Phys* 93:6724-6726.

Ikezoe Y, Hirota N, Nakagawa J, Kitazawa K (1998) Making water levitate. *Nature* 393:749-750.

Iwasaka M, Yamamoto K, Ando J, Ueno S (2003) Verification of magnetic field gradient effects on medium convection and cell adhesion. *J Appl Phys* 93:6715-6717.

Kishioka S, Yamada A, Aogaki R (2000) Analysis of gas dissociation rate into liquid phase under magnetic field gradient. *Phys Chem Chem Phys* 2:4179-83.

Kitazawa K, Hirota N, Ikezoe Y, Uetake H, Kaihatsu T, Takayama T (2002) Magneto-convection processes observed in non-magnetic liquid-gas system. *Riken Review* 44:156.

Kubitschek HE (1986) Increase in cell mass during the division cycle of *E. coli* B/rA. *J Bacteriol* 168:613-8.

Liu Y, Zhu D-M, Strayer DM, Israelsson UE (2010) Magnetic levitation of large water droplets and mice. *Adv Space Res* 45:208-213.

Lopez-Alcaraz P, Catherall AT, Hill RJA, Leaper MC, Swift MR, King PJ (2007). Magneto-vibratory separation of glass and bronze granular mixtures immersed in a paramagnetic fluid. *Eur Phys J E* 24:145.

Marrero TR, Mason EA (1972) Gaseous Diffusion Coefficients. *J. Phys. Chem. Ref. Data* 1:3-118.

Nakamura H, Takayama T, Uetake H, Hirota N, Kitazawa K (2005). Magnetically controlled convection in a diamagnetic fluid. *Phys. Rev. Lett.* 94:144501

Peng ZM, Wang J, Huang YJ, Chen QW (2004) Magnetic field-induced increasing of the reaction rates controlled by the diffusion of paramagnetic gases. *Chem Eng Technol* 27:1273.

Poodt PWG, Heijna MCR, Tsukamoto K, de Grip WJ, Christianen PCM, Maan JC, van Enckevort WJP, Vlieg E (2005) Suppression of convection using gradient magnetic fields during crystal growth of $NiSO_4.6H_20$. *Appl Phys Lett* 87:214105.

Poodt PWG, Heijna MCR, Christianen PCM, van Enckevort WJP, de Grip WJ, Tsukamoto K, Maan JC, Vlieg E (2006) Using gradient magnetic fields to suppress convection during crystal growth. *Cryst Growth Des* 6:2275-2280.

Qian A, S Di, Gao X, Zhang W, Tian Z, Li J, Hu L, Yang P, Yin D, Shang P (2009) cDNA microarray reveals the alterations of cytoskeleton-related genes in osteoblast under high magneto-gravitational environment. *Acta Biochim Biophys Sin* 41:561.

Simon MD, Geim AK (2000) Diamagnetic levitation: Flying frogs and floating magnets. *J Appl Phys* 87:6200-6204.

Steiner U, Ulrich T (1989) Magnetic field effects in chemical kinetics and related phenomena, *Chem Rev* 89: 51-147, and references cited therein.

Tanimoto Y, Fujiwara M, Sueda M, Inoue K, Akita M (2005) Magnetic levitation of plastic chips: applications for magnetic susceptibility measurement and magnetic separation. *Jpn J App Phys* 44:6801-6803.

Ueno S (1989) Quenching of flames by magnetic fields. *J. Appl. Phys.* 65:1243-1245

Ueno S and Iwasaka M (1994) Properties of diamagnetic fluid in high gradient magnetic fields. *J. Appl. Phys.* 75:7177-7179.

Valles JM Jr., Lin K, Denegre JM, Mowry KL (1997) Stable magnetic field gradient levitation of Xenopus laevis: toward low-gravity simulation. *Biophys J* 73:1130-1133.

Valles JM Jr. (2002) Model of magnetic field-induced mitotic apparatus reorientation in frogs eggs. *Biophys J* 82:1260-1265.

Valles JM Jr., Maris HJ, Seidel GM, Tang J, Yao W (2005) Magnetic levitation-based Martian and Lunar gravity simulator. *Adv Space Res* 36:114.

van Loon JJWA (2007) in *Biology in Space and Life on Earth. Effects of Spaceflight on Biological Systems*, ed Brinckmann E (Wiley-VCH Verlag CmbH & Co. KGaA, Weinheim), pp 17-32.

Weast R, ed. (1972) Handbook of Chemistry and Physics, 53rd ed, Cleveland Ohio, The Chemical Rubber Co.

Wilke CR, Chang P (1955) Correlation of diffusion coefficients in dilute solutions. *A.I.Ch.E. J.* 1:264-270.

Wilson JW, Ott CM, Honer zu Bentrup K, Ramamurthy R, Quick L, Porwollik S, Cheng P, McClelland M, Tsaprailis G, Radabaugh T, Hunt A, Fernandez D, Richter E, Shah M, Kilcoyne M, Joshi L, Nelman-Gonzalez M, Hing S, Parra M, Dumars P, Norwood K, Bober R, Devich J, Ruggles A, Goulart C, Rupert M, Stodieck L, Stafford P, Catella L, Schurr MJ, Buchanan K, Morici L, McCracken J, Allen P, Baker-Coleman C, Hammond T, Vogel J, Nelson R, Pierson DL, Stefanyshn-Piper HM, Nickerson CA (2007) Space flight alters bacterial gene expression and virulence and reveals a role for global regulator Hfq. *Proc Natl Acad Sci USA* 104:16299–16304.

Figures

Figure 1. Sedimentation and growth of cultures in the magnet

Samples of *E. coli*(pSB2999) culture in 25mm-diameter containers, expressing the green fluorescence protein, were grown in the magnet at 0*g**, 1*g** and 2*g** statically for 18 h at 37 °C and then visualized under UV illumination. The liquid depth is 15mm.

Figure 2. Growth of *E. coli* and *S. epidermidis*

Cultures of *E. coli* (Panel A) and *S. epidermidis* (Panel B) were grown at 37 °C in nutrient broth. They were either exposed to altered effective gravity in the magnet bore [(♦) 0*g**, (■) 1*g**, (▲) 2*g**] or were grown outside the magnet (1*g*) [(○) statically, (◊) aerated]. Samples were collected at hourly intervals in order to determine the cell density, using OD_{600nm}. Error bars show 1 standard deviation.

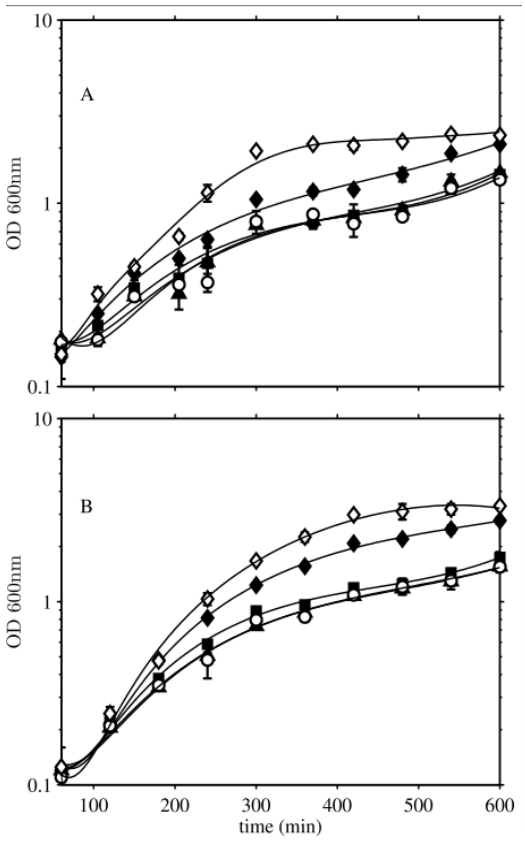

Figure 3. Relationship between final cell density and liquid-air interface area/sample volume.

Samples were incubated for 18 h in tubes with different dimensions (Table S1). The optical density (OD_{600nm}) after 18 h shows a clear increase with A/V; A is the area of the liquid-air interface and V is the sample volume. (a) OD of the $0g$* sample, OD($0g$*), relative to the OD of the $1g$* control sample in the magnet, OD($1g$*). (b) OD of the $0g$* sample, OD($0g$*), relative to the OD of the $1g$ control outside the magnet, OD($1g$). (c) OD of the $1g$ control. The scatter in the data points gives a good indication of the experimental uncertainty. Lines show the least-squares linear fit to the data. The gradients of the lines are, including standard errors, 8 ± 2, 11 ± 2 and 6.5 ± 1.0 μl mm^{-2}, for the data in panels A, B and C respectively.

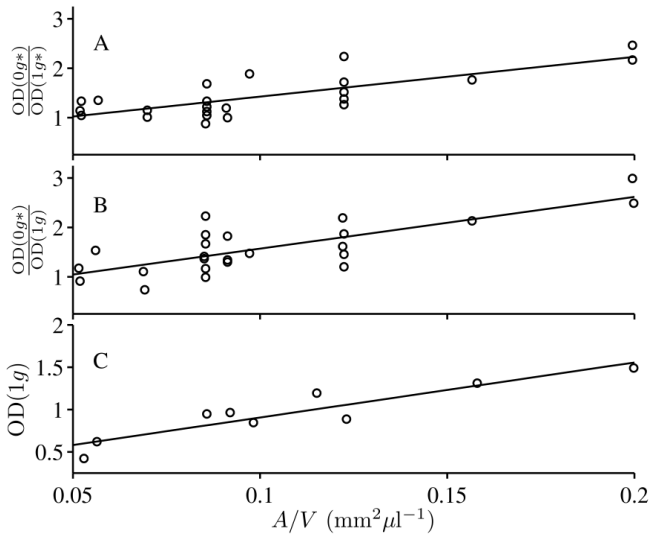

Figure 4. Magnetic convection in a bacterial culture

Static bacterial cultures (*E. coli*) in 10mm x 10mm x 45mm cuvettes, containing resazurin dye. The liquid depth is 12mm. Cuvettes in the 0*g** and 2*g** positions in the magnet, and 1*g* control outside the magnet, photographed *in situ* after 6 h. The dye turns pink in regions where bacteria are undergoing aerobic metabolism but have not become anaerobic, highlighting areas with a relatively high O_2 concentration. The image top right, labelled 'F', is a false-colour version of the 0*g** image shown top left. In this image, the shape of the O_2-depleted regions are coloured blue. The shapes of these regions are reminiscent of the shape of thermal convection cells.

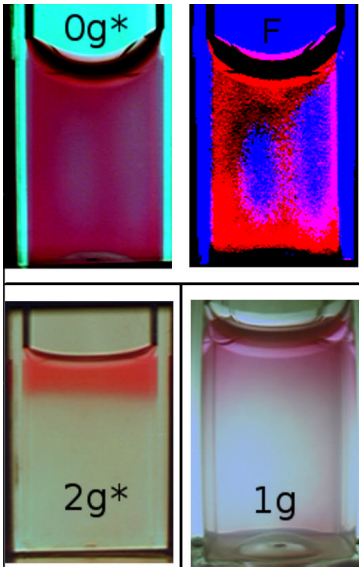

Tables

Table 1(a and b). Effects of culture conditions on cell growth.

Cultures were grown under different test conditions for 18 h at 37 °C in the 0*g**, 1*g** and 2*g** positions. The 1*g* control samples were grown outside the magnet either statically (1*g*) or with shaking (1*g* aerated). Optical density (OD_{600nm}) of samples was determined after 18h. Table 1a; final optical densities of cultures of *E. coli* grown without and with O_2-gassed perfluorodecalin (PFC) layer at the bottom of the culture. Table 1b; ratios of final cell density values of *E. coli* and *S. epidermidis* cultures. Only *E. coli* static cultures were oxygenated from the bottom of the culture by adding O_2-gassed PFC.

Table 1a

	Final cell density (OD_{600nm})	
Condition	**Without PFC**	**With PFC**
0*g**	1.9 ± 0.3	2.3 ± 0.1
1*g**	1.4 ± 0.1	1.9 ± 0.1
2*g**	1.3 ± 0.2	1.8 ± 0.1
1*g*	1.3 ± 0.1	1.8 ± 0.1
1*g* aerated	2.4 ± 0.2	n.d.

Table 1b

Test Comparison	*E. coli*	*E. coli* with PFC	*S. epidermidis*
0*g**/ 1*g*	1.73 ± 0.35	1.24 ± 0.05	1.94 ± 0.16
1*g**/ 1*g*	1.09 ± 0.03	1.06 ± 0.07	1.17 ± 0.25
2*g**/ 1*g*	1.04 ± 0.08	1.01 ± 0.02	0.73 ± 0.11
0*g** / 1*g**	1.59 ± 0.29	1.16 ± 0.03	1.53 ± 0.16
0*g** / 1*g* aerated	0.9 ± 0.05	n.d.	0.81 ± 0.02

n.d, not done

Table 2. Microarray analysis of changes in expression of cytochromes and *fnr*

Comparison of significant fold changes in expression for genes involved in cytochrome regulation in *E. coli* K12 MG1655. Samples were exposed to altered effective gravity at 37 °C in the magnet bore (0*g**, 1*g** or 2*g**) or grown outside the magnet (1*g*) either statically or aerated. All samples were harvested at OD_{600nm} = 0.5 for RNA extraction to minimize effects caused by changes in cell population and associated depletion of gases and nutrients. Total RNA was extracted from 4 independent replicates and used for microarray analysis. Data were analyzed using GeneSpring GX 7.3, and normalized against 50% of signal for each independent array and filtered using p-value = 0.05.

Test conditions	Gene	Gene Product	Fold change
0*g vs. 1*g****	*cyoA*	cytochrome o ubiquinol oxidase subunit II	2.11
	cyoB	cytochrome o ubiquinol oxidase subunit I	2.34
	appA	phosphoanhydride phosphorylase	0.47
	appC	cytochrome bd-II oxidase, subunit I	0.45
0*g vs. 2*g****	*cyoB*	cytochrome o ubiquinol oxidase subunit I	2.98
	appB	cytochrome bd-II oxidase, subunit II	0.33
	appC	cytochrome bd-II oxidase, subunit I	0.2
	Fnr	DNA-binding transcriptional dual regulator, global regulator of anaerobic growth	0.43
0*g vs. 1*g***	*cyoD*	cytochrome o ubiquinol oxidase subunit IV	2.12
	cyoE	Protoheme IX farnesyltransferase	2.12
	Fnr	DNA-binding transcriptional dual regulator, global regulator of anaerobic growth	0.37
1*g vs. 1*g* aerated**	*cyoB*	cytochrome o ubiquinol oxidase subunit I	0.42
1*g vs. 2*g****	*appB*	cytochrome bd-II oxidase, subunit II	0.47
	appC	cytochrome bd-II oxidase, subunit I	0.4

Table 3. Comparison of qRT-PCR and microarray data for *cyoA* and *appB*

Samples of RNA extracted for the array experiments from 4 independent replicates of cells grown in altered effective gravity at 37°C in the magnet bore (0*g*,* 1*g** or 2*g**) or statically outside the magnet (1*g*), were used for qPCR analysis. Cells were recovered from each culture for RNA extraction when OD_{600nm} = 0.5. Levels of *cyoA* and *appB* were compared in each case with the 1*g* control sample. Details of TaqMan probes and dyes used are provided in Table S3. Values that were statistically different at the 5% level from a 1:1 ratio are indicated by * .

Test conditions	**Fold change**			
	cyoA		***appB***	
	Arrays	**qRT-PCR**	**Arrays**	**qRT-PCR**
0*g** /1*g*	1.49*	1.57*	0.69	0.80
1*g**/1*g*	0.71	0.90	0.88	0.92
2*g** /1*g*	0.95	0.80	1.82*	2.20*

* p values < 0.05

Diamagnetic levitation enhances growth of liquid bacterial cultures by increasing oxygen availability: *Electronic Supplementary Material*

Camelia E. Dijkstra[1], Oliver J. Larkin[1], Paul Anthony[1], Michael R. Davey[1], Laurence Eaves[2], Catherine E. D. Rees[1], Richard J. A. Hill[*,2]

[1] School of Biosciences, University of Nottingham, Sutton Bonington Campus, Loughborough, LE12 5RD, UK.

[2] School of Physics and Astronomy, University of Nottingham, Nottingham, NG7 2RD, UK.

* email: richard.hill@nottingham.ac.uk.

S1 MAGNETIC LEVITATION

S1.1 Effective gravity on-axis

Consider the forces acting on a small volume dV of material at a point (x, z) in the magnetic field; x and z are radial and vertical coordinates, with origin at the geometric centre of the solenoid. The net vertical force, i.e. the sum of the gravitational and vertical magnetic forces, acting on this volume, is $F = (\chi B B_z'/\mu_0 - \rho g)dV$ (Beaugnon & Tournier 1991, Berry & Geim 1997, Valles et al. 1997, Simon & Geim 2000). Here, B and $B_z' = \partial B/\partial z$ are the magnitude of the magnetic field and the magnetic field gradient at the point (x, z), respectively; χ and ρ are the volume magnetic susceptibility and density of the material, respectively; $g = 9.8$ ms^{-2} and $\mu_0 = 4\pi \times 10^{-7}$NA^{-2}. The term in F proportional to BB_z' is the magnetic force and $\rho g dV$ is the gravitational force, i.e. the weight. For material on the vertical solenoid's axis, the net force points vertically: there is no radial component of the force. When the magnetic force balances the gravitational force, i.e. when $F = 0$, the material levitates. Water, which has $\chi_w = -9 \times 10^{-6}$ (S.I. units) and $\rho_w = 1000$ kg m^{-3}, levitates approximately 75-80 mm above the geometric centre of our solenoid (depending on the solenoid current), where $BB_z' = -1370$ T^2 m^{-1} and B = 12.3 T (the negative value of BB_z' indicates that B decreases with increasing height above the centre of the solenoid). We define the effective gravity acting on the water as $\Gamma_z = F/\rho dV = \chi B B_z'/(\rho\mu_0) - g$. At the levitation point, $\Gamma_z = 0$. Notice that a

positive value of Γ_z indicates a net *upward* force, and a *negative* value of Γ_z indicates a net *downward* force.

S1.2 Effective gravity off-axis

Away from the solenoid axis, the magnetic field has a non-zero radial component. Hence, the effective gravity has a radial component, off-axis, too, $\Gamma_x = \chi B B_x'/(\rho\mu_0)$, where $B_x' = \partial B/\partial x$ is the radial component of the magnetic field gradient. The effective gravity *vector* is $\mathbf{\Gamma} = \Gamma_x \boldsymbol{i} + \Gamma_z \boldsymbol{k} = \chi B \nabla B/(\rho\mu_0) - g\boldsymbol{k}$, where $\boldsymbol{k}$ is a unit vector pointing vertically upward, aligned with the solenoid axis, and $\boldsymbol{i}$ is the radial unit vector, perpendicular to $\boldsymbol{k}$.

S1.3 Stability of levitation

Stable diamagnetic levitation of liquid water is possible using this magnet (Hill & Eaves 2008, 2010. See also, Beaugnon et al. 2001). Close to the point of stable levitation, which we label L_0 [Hill & Eaves (2010)], $\mathbf{\Gamma}$ points inward toward L_0; for a discussion of the stability of diamagnetic levitation see Berry and Geim (1997) and Simon and Geim (2000). At L_0, water levitates stably, without need for a container. Beneath this point there is a second, *unstable* levitation point, L_1. The distance between the two points depends on the current in the solenoid. Near L_1, the radial component of $\mathbf{\Gamma}$ points toward L_1, but the vertical component of $\mathbf{\Gamma}$ points downwards. For the experiments in this paper, we have lowered the solenoid current below that required for stable levitation, leaving only the unstable L_1 point, as shown in Fig. S1. Although water (and the culture medium) levitates at L_1 (i.e. the magnetic and gravitational forces are balanced), it will fall without a container. We use this configuration for these experiments, rather than a stable levitation configuration, for simplicity: there is one levitation point, rather than two.

S1.4 Variation in effective gravity within the sample containers

At the geometric centre of the solenoid $\Gamma_z = 1g$ since $BB_z' = 0$ here. Note that the field is $B = 16.3$ T, here. Approximately 75mm below the centre, there is a $\Gamma_z = 2g$ point, where gravity and the magnetic force are additive. Three sample containers (25ml volume) are placed enclosing each of the three positions, and labelled "$0g$*", "$1g$*" and "$2g$*" as discussed in Sect. 3 (main text). The effective gravity within each sample

container varies due to the spatial variation of BB_z' as discussed above. The variation of Γ in the $0g^*$ container is shown in Fig. S1. The magnitude of $\mathbf{\Gamma}$ is zero at L_1, and increases with distance away from it, as shown in Fig S1. The maximum value of $|\mathbf{\Gamma}|$ within a 5mm radius of L_1 is 0.04g. Within a 10mm radius, the maximum is 0.10g. In all experiments, we limit the volume of the culture in the sample containers so that the effective gravity within the liquid culture varies by less than 10%.

S2 BUOYANCY OF CELLS IN LEVITATING CULTURE MEDIUM

S2.1 Effective gravity acting on the cells in the culture

Whether an individual cell floats or sinks in the liquid culture medium depends on Archimedes' principle, i.e. on the difference between the cell's weight and the weight of fluid displaced by the cell. In a weightless environment, e.g. in an orbiting spacecraft, both weights are zero, so the cells are neutrally buoyant.

The net vertical force on a cell in the magnetic field is, including the buoyancy forces, $F_z^{(c)} = \Delta\chi V B B_z'/\mu_0 - \Delta\rho V g$ (Catherall et al. 2005), where $\Delta\chi = \chi_c - \chi_w$ and $\Delta\rho = \rho_c - \rho_w$. Here, χ_c is the spatially-averaged volume magnetic susceptibility of the cell, V is the cell volume and ρ_c is the spatially-averaged ('buoyant') density of the cell (i.e. its mass divided by V). From this force, we define an effective gravity acting on the cell $\Gamma_z^{(c)} = \Delta\chi B B_z'/(\rho_c\mu_0) - g\Delta\rho/\rho_c$. Note that this effective gravity gives the net force on the *whole* cell $F_z^{(c)} = \rho_c V \Gamma_z^{(c)}$; within the cell, there is some variation in the magnetic and gravitational forces due to variations between the susceptibility and density of the cell's constituents (Valles et al. 1997). For neutral buoyancy, we require the net force acting on the cell to be zero; that is, we require $\Gamma_z^{(c)} = 0$.

Note that BB_z' does not vary significantly within the volume of the cell; the maximum spatial variation in BB_z' is $\sim 20\mathrm{T}^2\mathrm{m}^{-1}$ per mm within the levitating culture. Hence, for simplicity, we can assume that BB_z' is a constant within the cell.

S2.2 Sedimentation rate of cells

By equating $F_z^{(c)}$ with the Stokes' drag force on a cell moving through the liquid culture medium $F_\mathrm{s} = -6\pi\eta r u$, we obtain an estimate of the sedimentation velocity u. Here, r is the radius of a sphere having the same volume as the cell and $\eta = 1 \times 10^{-3}$ Pa.s is the

dynamic viscosity of the medium. However, since u depends on the cell radius (which changes during the life of the cell), it is more informative to determine $u(0g^*)/u(1g)$, i.e. the ratio of the sedimentation rate in 0g* to that outside the magnet, which is independent of r. We find $u(0g^*)/u(1g) = \Gamma(0g^*)/\Gamma(1g) = 0.1 \pm 0.3$. Here, Γ is the effective gravity acting on the cell, $\Gamma_z^{(c)}$, as defined above.

See main article for list of ***references***

Figure S1. Effective gravity Γ within the 25 ml specimen tube at the 0*g** position. The internal diameter of the tube is 25mm. The contours show the magnitude of Γ. The contour labels give the magnitude of the effective gravity as a percentage of 1*g*, i.e. they show 100Γ/*g*, where g=9.8ms^{-2}. The region Γ<0.1*g* is shown in blue. The arrows show the direction of the effective gravity vector **Γ**. The container is filled with liquid to the height indicated by the dashed yellow line. The levitation point, i.e. the point where the diamagnetic force balances the gravitational force, is labelled L_1. The magnetic field profile, used to construct this plot, was computed by numerical integration of the Biot Savart integral, using a thin-shell approximation for the current density in the solenoid.

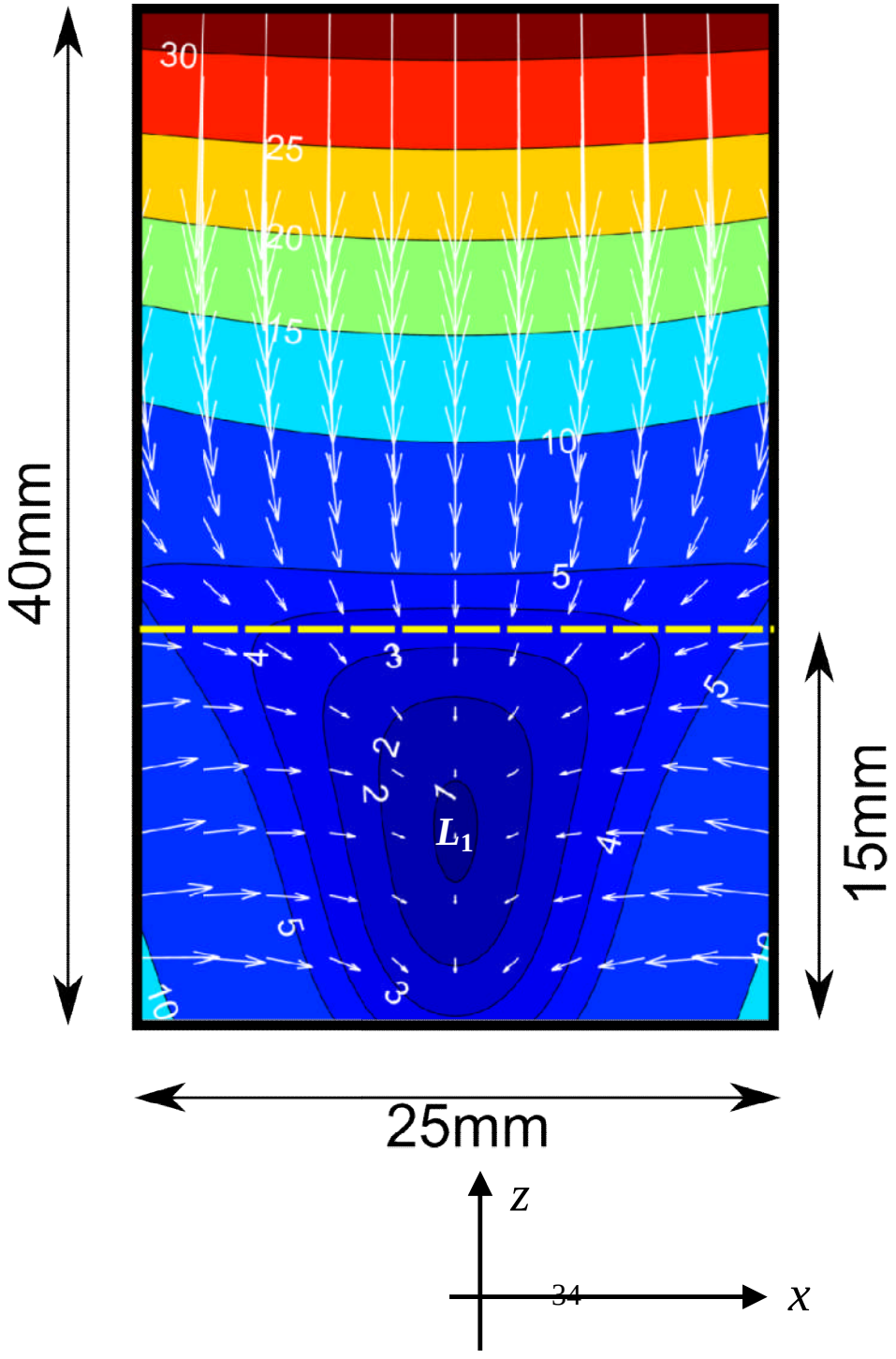

Figure S2. A) Schematic of the cryostat housing the solenoid magnet. The 5cm-diameter bore and the superconducting solenoid are indicated. B) Photograph of the top plate of the cryostat showing the entrance to the bore.

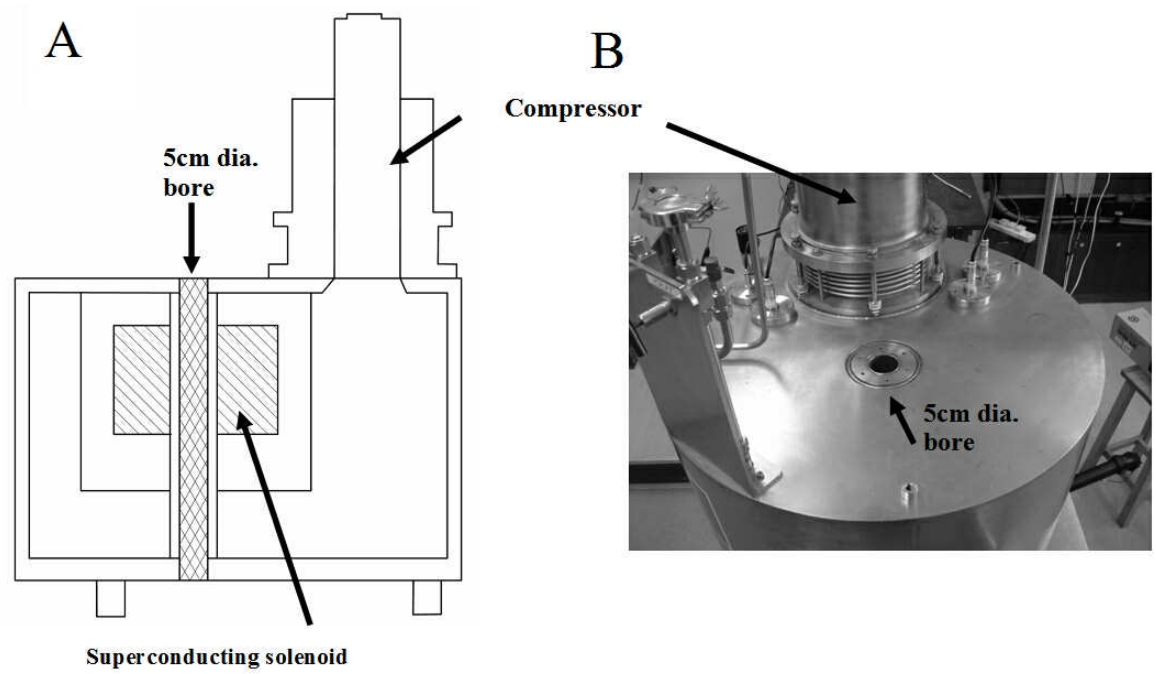

Figure S3. Temperature-regulated chamber containing three specimen tubes. i) frame used to hold specimen tubes in the 0g*, 1g* and 2g* positions within the magnet. Specimen tubes are supported by nylon collars attached to three threaded brass rods. The position of the collars is adjustable. White LED lighting and web cameras, stripped of ferromagnetic components, were installed to obtain images of the samples *in situ*. Thermocouples, connected to a data logger, were installed to monitor the temperature of each sample. ii) frame located within the temperature-regulated chamber; air-flow ports can be seen top and bottom. The air supply is passed through a heat exchange coil immersed in a thermostatically-controlled water bath.

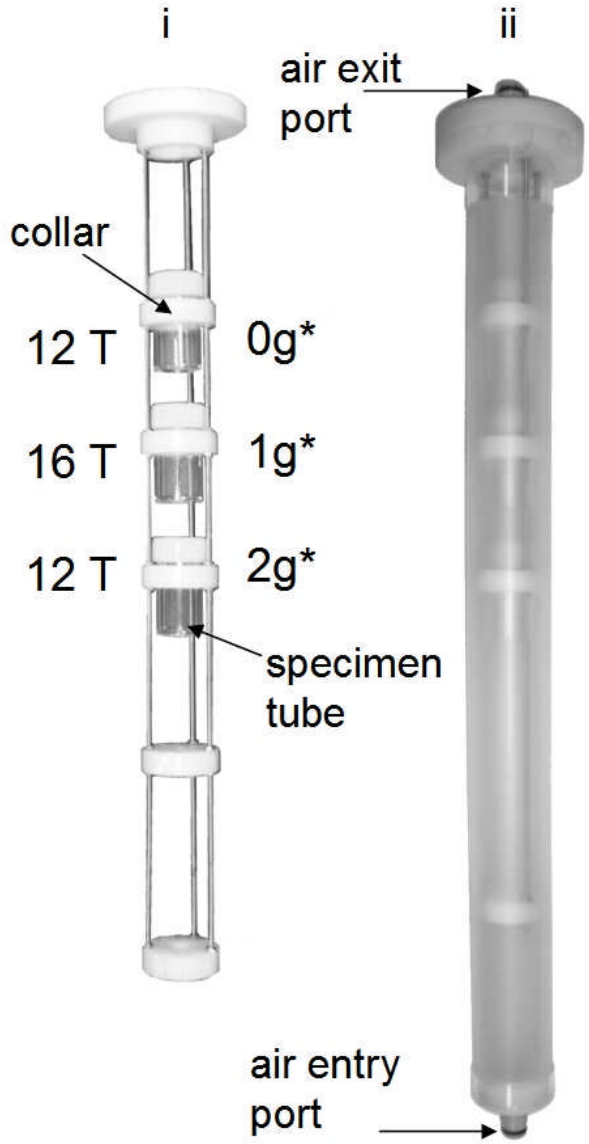

Table S1 Dimensions of the culture vessels used within the magnet bore

Container	Volume (µl)	Surface area vs. Volume($mm^2 µl^{-1}$)
0.2ml		
Tubes	**100**	**0.200**
	200	**0.115**
	300	**0.085**
0.5ml		
Tubes	**200**	**0.157**
	350	**0.092**
	600	**0.056**
	700	**0.053**
25ml		
Tubes	**700**	**0.698**
	4000	**0.122**
	5000	**0.098**

Table S2. Comparison of significant fold changes (p < 0.05) in expression for genes involved in cytochrome regulation in *E. coli* K12 MG1655.

Test conditions	Gene	Gene Product	Fold change
0*g vs. 1*g****	*cyoA*	cytochrome o ubiquinol oxidase subunit II	2.11
	cyoB	cytochrome o ubiquinol oxidase subunit I	2.34
	ndh	respiratory NADH dehydrogenase, aerobic respiration	2.41
	appA	phosphoanhydride phosphorylase	0.47
	appC	cytochrome bd-II oxidase, subunit I	0.45
0*g vs. 2*g****	*cyoB*	cytochrome o ubiquinol oxidase subunit I	2.98
	appB	cytochrome bd-II oxidase, subunit II	0.33
	appC	cytochrome bd-II oxidase, subunit I	0.20
	ppa	inorganic pyrophosphatase (phosphorus metabolism)	0.35
	fnr	DNA-binding transcriptional dual regulator, global regulator of anaerobic growth	0.43
0*g vs. 1*g***	*cyoD*	cytochrome o ubiquinol oxidase subunit IV	2.12
	cyoE	protoheme IX farnesyltransferase	2.12
	atpC	F1 sector of membrane-bound ATP synthase, epsilon subunit (ATP synthesis coupled proton transport)	2.10
	fnr	DNA-binding transcriptional dual regulator, global regulator of anaerobic growth	0.37
1g* vs. 1*g* aerated	*cyoB*	cytochrome o ubiquinol oxidase subunit I	0.42
1*g vs. 2*g****	*appB*	cytochrome bd-II oxidase, subunit II	0.47
	appC	cytochrome bd-II oxidase, subunit I	0.40
	ppa	inorganic pyrophosphatase (phosphorus metabolism)	0.34
1*g* vs. 2*g**	*frdC*	fumarate reductase (anaerobic),	0.25
	frdD	fumarate reductase (anaerobic),	0.42
	ppa	inorganic pyrophosphatase (phosphorus metabolism)	0.41
	atpC	F1 sector of membrane-bound ATP synthase, epsilon subunit (ATP synthesis coupled proton transport)	0.47
1g vs. 1*g* aerated	*cyoE*	protoheme IX farnesyltransferase	0.48

To ensure changes seen were due to suspension of cells, changes in expression due to the magnetic field alone (comparison of 1*g** and 1*g* results) were removed from analysis. Samples were exposed to altered effective gravity at 37 °C in the magnet bore (0*g**, 1*g** or 2*g**) or grown outside the magnet (1*g*) either statically or aerated. All samples were harvested at OD_{600nm} = 0.5 for RNA extraction to minimize effects caused by changes in cell population and depletion of gases and nutrients. Total RNA was extracted from 4 independent replicates and used for microarray analysis. Data were analyzed using GeneSpring GX 7.3, and normalized against 50% of signal for each independent array and filtered using p-value = 0.05.

Table S3. Primers and probes used for qRT-PCR analysis

Gene	Forward Primer	Reverse Primer
appB	GGAGTATCTCGGCAGCTTCTG	GCTGAGCAATCCGCACAATAAAG
envZ	CCCGGCAGCATTGAAGTGA	CCACCGCGCGTTTGATC
cyoA	CGAGAAGCCCATTACCATCGAA	CCTGTTCCGGGTAGATGAAGAA

Reporter 1 Name	Reporter 1 Dye	Reporter 1 Sequence
APPB-AP1M1	FAM	CTGCTGACGCCATTCC
ENVZ-EN4M2	FAM	ACAGCGGGTGCATTT
CYOA-CO1M2	FAM	CCAGTCCATGGAAACCA